Conformer-Dependent Proton-Transfer Reactions of Ubiquitin Ions

Stephen J. Valentine, Anne E. Counterman, and David E. Clemmer
Department of Chemistry, Indiana University, Bloomington, Indiana, USA

The conformations of ubiquitin ions before and after being exposed to proton transfer reagents have been studied by using ion mobility/mass spectrometry techniques. Ions were produced by electrospray ionization and exposed to acetone, acetophenone, n-butylamine, and 7-methyl-1,5,7-triazabicyclo[4.4.0]dec-5-ene. Under the conditions employed, the +4 to +13 charge states were formed and a variety of conformations, which we have characterized as compact, partially folded, and elongated, have been observed. The low charge state ions have cross sections that are similar to those calculated for the crystal conformation. High charge states favor unfolded conformations. The ion mobility distributions recorded after ions have been exposed to each base show that the lowest charge state that is formed during proton-transfer reactions favors a compact conformation. More open conformations are observed for the higher charge states that remain after reaction. The results show that for a given charge state, the apparent gas-phase acidities of the different conformations are ordered as compact < partially folded < elongated. (J Am Soc Mass Spectrom 1997, 8, 954–961) © 1997 American Society for Mass Spectrometry

The development of electrospray ionization (ESI) [1] and matrix assisted laser desorption ionization (MALDI) [2] for mass spectrometry (MS) has made it possible to produce large biological ions in the gas phase. The structures and stabilities of these ions have recently received considerable attention, because they can provide information about the intrinsic nature of these species in the absence of solvent. Several methods have been used to investigate the conformations of gas-phase proteins, including gas-phase H/D exchange [3–6], proton-transfer reactions [5, 7–9], measurements of average collision cross sections [6, 10–13], and microscopy studies of the hillocks formed on surfaces after high-energy ion impacts [14]. Many of these studies provide evidence that conformations of gas-phase protein ions are influenced by the number of charges that are accommodated during the ESI process [9, 10, 12, 14]. Highly charged ions appear to favor conformations that are elongated instead of compact because of lower Coulombic repulsion energies. Low charge states can exist in more compact forms. Several recent studies have shown that when high charge states are exposed to proton-transfer reagents, the lower charge states that are formed appear to have folded conformations, demonstrating that proteins can fold in the gas phase [4b, 9b, 12b, 13].

In this article we have examined the conformations of ubiquitin ions before and after they have been exposed to four proton-transfer reagents by using ion mobility/mass spectrometry techniques [15]. The mobility of a protein ion in the gas phase depends on its average collision cross section with a buffer gas. Compact conformers have smaller cross sections and thus higher mobilities than elongated ones [12]. By comparing ion mobility data and mass spectra for ubiquitin ions before and after exposure to proton-transfer reagents, we have examined the changes in the distributions of conformations that occur within different charge states during proton-transfer reactions. Several studies have drawn correlations between the proton affinity of multiply charged ions and the total Coulomb energy [9a, 16]. These results imply that for a given charge state elongated conformations will be less reactive than compact ones because the former species have lower Coulomb energies. The present experiments provide direct structural information about lower charge states, formed by proton-transfer reactions, and high charge states that remain after exposure to different bases.

We have chosen to investigate the reactions of ubiquitin ions (bovine) with acetone, acetophenone, n-butylamine, or 7-methyl-1,5,7-triazabicyclo[4.4.0]dec-5-ene (MTBD) for several reasons. First, ubiquitin is a relatively small and simple protein. It is comprised of 76 amino acids and has 12 basic lysine, arginine and histidine residues. Ubiquitin contains no disulfide bonds and should be relatively free to adopt different conformations according to differences in coulomb energy. Second, the proton transfer reactivity of ubiquitin

Address reprint requests to D. E. Clemmer, Dept. of Chemistry, Indiana University, Bloomington, IN 47405.

1044-0305/97/$17.00
PII S1044-0305(97)00085-8

Received January 29, 1997
Revised April 9, 1997
Accepted April 11, 1997

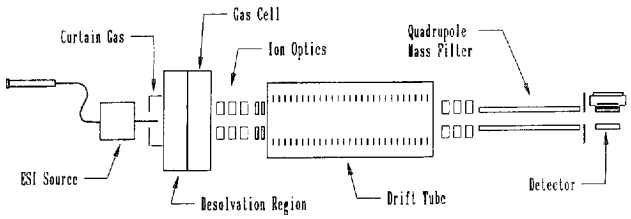

Figure 1. Schematic diagram of the experimental apparatus.

has been examined previously [5, 7, 8b]. Several charge states show evidence of multiple conformers and apparent gas-phase acidities for different charge states have been reported [8b]. The role of the solution conformation on the gas-phase reactivity has also been investigated [7]; however, no differences in the reactivity of the gas-phase ions from different solution conditions have been observed. Finally, the proton-transfer bases were chosen because they provide a wide range of gas-phase basicities. The reaction enthalpy for each charge state varies with each proton transfer base, such that it is possible to examine reaction channels that are allowed for some bases but inaccessible for others. This allows us to establish the relative ordering of the thermochemistry for different conformations. We report the ordering in terms of apparent gas-phase acidities in order to be consistent with the thermochemistry reported by Zhang and Cassady [8b]. They have previously delineated the relationship of the free energy change of proton transfer reactions to apparent gas-phase acidities and basicities [8b].

Experimental

General

A schematic diagram of our experimental apparatus is shown in Figure 1. Multiply charged ubiquitin ions were formed by electrospraying a 1:1 water:acetonitrile solution containing 8.0×10^{-5} M ubiquitin (bovine, Sigma, St. Louis, MO, 90%) and 2.0% acetic acid. Electrosprayed droplets are formed at atmospheric pressures and enter a variable temperature, differentially pumped desolvation region through a 0.1-cm-diameter entrance orifice. The ions pass through this region and exit through a 0.1-cm-diameter exit aperature, where they enter the source gas cell. Here, proton transfer reagents can be introduced as described below. The diameters of entrance and exit aperatures can be varied easily. The pressure in each region is ~1–10 torr depending on which apertures are used. Protein ions are extracted from the reaction cell into a high vacuum region (10^{-4} to 10^{-5} torr), focused into a low-energy ion beam, and injected into the drift tube. As shown below, the injection energy can influence the distribution of conformations. Except where noted, these experiments are carried out at an injection energy of 385 eV. For large ions, this is a low injection energy that favors conformations that are present in the ion source. At higher injection voltages, elongated conformations that are formed at the entrance of the drift tube are favored.

The drift tube is 32.4 cm long and contains ~2 torr of 300 K helium buffer gas. The entrance and exit apertures are 0.08 cm in diameter and 26 equally spaced electrostatic lenses ensure a uniform electric field along the axis of the ion beam. The drift tube body is made of stainless steel with Teflon® spacers at each end, which electrically isolate the entrance and exit plates. In these studies, a drift field of 13.9 V cm^{-1} was used. After exiting the drift tube, ions are focused into a quadrupole mass spectrometer that can be set to transmit a specific mass (for measurements of ion mobility distributions) or scanned in order to monitor product formation.

Conformer Separation

In order to separate different conformers, 30–50 μs pulses of ions were injected into the drift tube and the arrival time distribution at the detector was recorded using a multichannel scaler. Different protein conformations within a given charge state are separated because of differences in their mobilities through the buffer gas [12]. Compact conformers with small collision cross sections have higher mobilities than larger conformations. As in electrophoresis, the mobility also depends on the charge state. High charge states have larger mobilities than low charge states because of differences in the effective drift field ($E_{eff} = zV/L$, where V is the applied drift voltage, L is the length of the drift tube, and z is the charge state of the protein ion). For comparison of different charge states, it is useful to plot data on a modified t^*z timescale that normalizes for differences in effective field.

The experimentally measured arrival time is a composite of the time the ions spend in the drift tube and the time required for the ion pulse to travel through other portions of the instrument before reaching the detector. Thus, it is necessary to subtract the flight time of the ions when no buffer gas is present and also account for differences in the ions' kinetic energies at the exit of the drift tube, with and without buffer gas. In these studies, the differences between the arrival times and drift times were between 250 and 350 μs.

Collision Cross Sections

Orientationally averaged collision cross sections can be derived directly from the ion mobility distributions using the relation [17]

$$\Omega = \frac{(18\pi)^{1/2}}{16}\frac{ze}{(k_BT)^{1/2}}\left(\frac{1}{m_T}+\frac{1}{m_B}\right)^{1/2} \times \frac{t_DE}{L}\frac{760}{P}\frac{T}{273.2}\frac{1}{N}, \quad (1)$$

where t_D is the average drift time, E is the electric field, P is the pressure in torr, z is the charge state, N is the neutral number density, and m_I and m_B are the masses of the ion and buffer gas, respectively. This equation can be rearranged to solve for the drift time under a specific set of experimental conditions, which is useful for predicting where assumed conformations might appear in the ion mobility distributions, as discussed below. All of the parameters E, L, P, and t_D can be precisely measured. Thus, the reproducibility of measured cross sections in these studies is excellent, with different measurements usually agreeing to within 1%.

Proton-transfer Reactions

Proton-transfer reactions are studied by comparing mass spectra and ion mobility distributions taken before a base is added to the reaction cell to data taken after the base has been introduced. Bases [acetone (Aldrich, 99.5%), acetophenone (EM Science, 98%), n-butylamine (Mallinckrodt Chemical, 96%), or MTBD (Aldrich, 98%)] were added by carefully monitoring the ion signal while introducing base vapor through a leak valve. Addition of the base causes dramatic changes in the signals of individual charge states and at the first sign of a change in signal, the setting on the leak valve was decreased slightly and we began collecting data. Under these conditions, the partial pressure of the base could not be discerned from the background pressure of the gas cell (~1 to 10 torr). Mass spectra, acquired before and after base was added to the gas cell, confirm that proton-transfer reactions have occurred as discussed below.

In a limited number of experiments, we have removed the source gas cell and drift tube and recorded mass spectra directly from the source. These studies show that ions are efficiently desolvated in the ion source. Thus, we assume that reactions in the source gas cell involve solvent-free protein ions and the reagent base. The internal (i.e., vibrational and rotational) and kinetic energy distributions of our ions in this region are unknown, but should be similar for different conformations.

Conformer Identification

Experimental drift times and cross sections can be compared with calculated cross sections for trial protein conformations. In this study, we compare our data to the crystal form of ubiquitin [18] as well as a near-linear form of the protein created using the Insight II molecular modeling software [19]. The orientationally averaged projection of the protein is calculated as described previously [12b, 13]. This approach gives only an approximation of the true cross section because it assumes only elastic hard-sphere collisions between the buffer gas and the protein and does not rigorously account for the protein-He scattering trajectories [20] or conformational dynamics of the protein as it travels through the gas. However, for the purposes of the present work, it provides an adequate comparison. The average hard-sphere projection cross sections are 897 and 2140 Å^2 for the trial crystal and near-linear conformations, respectively.

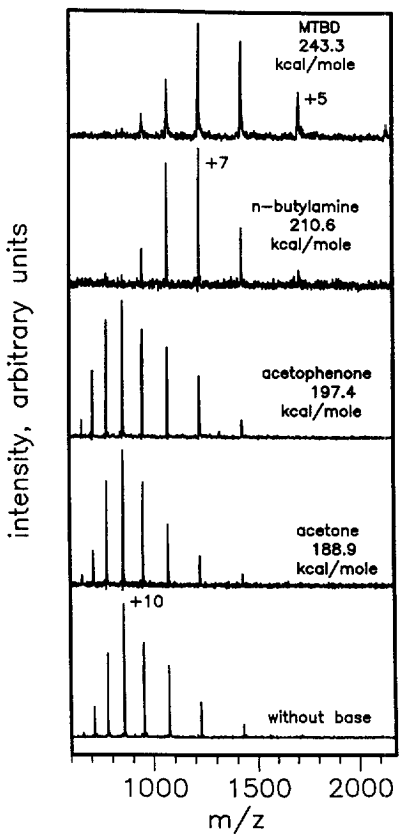

Figure 2. Mass spectra for ubiquitin before and after proton-stripping reagents have been added to the source gas cell.

Results and Discussion

Proton-transfer Mass Spectra

Prior ESI mass spectra of ubiquitin measured by Loo and co-workers have shown that the charge state distribution depends on the properties of the solution [7]. Native solutions favor the +6 to +8 charge states, while solutions containing organic solvent and acids favor higher charge states. Exposing the ions to trimethylamine [Gas phase basicity (GB) = 217.3 kcal/mol] [21] in a reagent inlet near the ESI source results in spectra that are dominated by the +6 state for both solutions [7].

Figure 2 shows our mass spectra for ubiquitin ions formed directly by ESI, and data recorded after ions were exposed to acetone, acetophenone, n-butylamine, or MTBD in the source gas cell. Before bases are added, we observe the +6 to +13 charge states of ubiquitin and the dominant charge state is the +10, similar to previous results [7]. After proton-transfer reagents are added to the gas cell, lower charge states are favored in the

mass spectra. Addition of acetone, with a gas-phase basicity (GB) of 188.9 kcal/mol [22], has little effect on the overall distribution of charge states. When acetophenone (GB = 197.4 kcal/mol), n-butylamine (GB = 210.6 kcal/mol), and MTBD (GB = 243.3 kcal/mol) [23] are added, lower charge states are favored, including the +5 state (observed for n-butylamine and MTBD) and +4 (observed only for MTBD). The shifts in charge state distributions indicate that proton-transfer reactions have occurred.

Ion Mobility Distributions Before Proton-Transfer Reactions

By varying the energy that is used to inject ions into the drift tube, it is possible to observe different conformations in the ion mobility distribution. As ions enter the drift tube they are rapidly heated as their kinetic energies are thermalized by collisions with the buffer gas. Further collisions ($\sim 10^5$ per cm) cool the ions to the buffer gas temperature. Most of the ion mobility distributions discussed here were recorded using an injection energy of 385 eV, a low-energy condition that is expected to reflect the distributions of conformers in the source. This injection energy was chosen because ample ion signals for these studies exist for all charge states. For some states it was possible to record ion mobility distributions at lower injection energies. These data are similar to those recorded at 385 eV, indicating that the distributions reflect the population of different conformers in the source.

We have carried out ion mobility studies for the +6 to +13 charge states. Detailed injection energy studies for the +6 to +10 charge states, before ions are exposed to proton-transfer reagents are shown in Figure 3. Ion mobility distributions for the +11 to +13 states have also been recorded and display single peaks similar to those shown for the +10 state. However, the ion signals are much smaller and the data are not shown. At 385 eV, multiple features are clearly observed in the ion mobility distributions for the +6 to +8 charge states and the +9 state displays a small shoulder at 15.5 ms in addition to the large peak at slightly longer times. This shows that multiple conformations are present for these states. The most compact conformation observed for the +6 state at low injection energies has a drift time of 10.9 ms, which is similar to the 9.4 ms value calculated for the crystal structure. At high injection energies, the distributions for all charge states show only a single peak, having the same drift time as the peak at longest times in each distribution recorded at low injection energies. No dissociation is observed at these injection energies. Therefore, changes in the relative abundances of peaks indicates changes in the fractions of different conformations. In this case, all of the more compact forms of the +6 to +9 states must have unfolded to a more open structure for each charge state.

The peak observed in data recorded at high energies

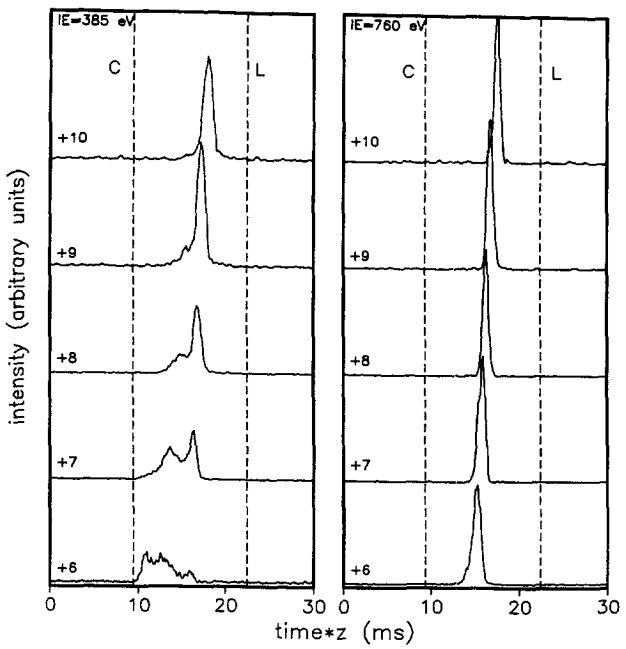

Figure 3. Ion mobility distributions at low (385 eV) and high (760 eV) injection energies for the +6 to +10 charge states of ubiquitin. Distributions are shown on a charge-normalized t^*z timescale that normalizes for differences in the effective field strength for different charge states. The dashed lines at 9.4 and 22.4 ms are the calculated drift times for the crystal and near-linear model conformations.

is notably narrower than the analogous feature observed at low injection energies. Comparison of these data to the distribution calculated for transport of a single conformation [17] shows that both experimental peaks are significantly broader than expected for a single conformer (by factors of ~3 and ~2 at low and high injection energies, respectively). This indicates that either multiple elongated conformations (which are not entirely resolved by our experiment) are present, or that conformations are interconverting as they travel through the drift tube. Cassady and Carr have resolved two conformations of the +12 state of ubiquitin based on different H/D exchange levels and proton transfer rates [5]. The proton-transfer data also show that multiple conformations are present for the +4 to +6 states, but only a single conformation was observed for remaining states (i.e., +7 to +11, and +13). Our current data show evidence that multiple conformers can exist for all charge states.

Experimental Cross Sections

Figure 4 shows collision cross sections that were derived using eq 1 for the features observed in the ion mobility data. This plot includes conformers observed after proton-transfer reactions (shown below). Many of the ion mobility distributions show broad unresolved features. This prevents us from deriving precise collision cross sections for all of the conformations that must

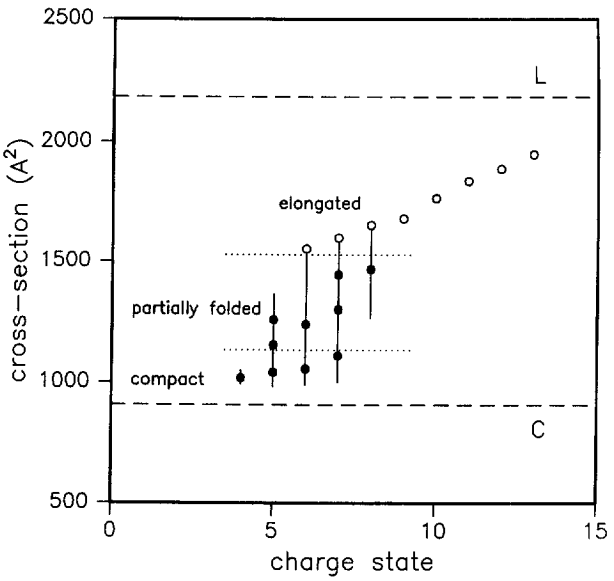

Figure 4. Experimental collision cross sections for all conformations and charge states observed for ubiquitin. The vertical lines correspond to a distribution of unresolved conformations having a range of collision cross sections. The filled circles that are superimposed on the lines correspond to reproducible maxima in the unresolved spectra. The dashed lines correspond to the calculated cross sections for the crystal conformer (C) and the near-linear conformer (L). Dotted lines are used to divide the data into three conformer types: compact, partially folded, and elongated.

be present. The narrow peak observed at high injection energies (+6 to +13) gives the largest collision cross section observed for each charge state. As the charge state increases from +6 to +13, the experimental collision cross sections increase from 1525 Å^2 for the +6 charge state to a maximum of 1912 Å^2 for the +13 charge state. This increase is comparable to the increase observed in the most open forms of multiply charged cytochrome *c* [10a, 12a], apomyoglobin [12d], and lysozyme [13], and shows the effect of increasing Coulombic repulsion on conformation. As the Coulomb energy increases, the cross sections approach the value calculated for a near-linear conformation, showing that they are extremely elongated.

The vertical lines shown in Figure 4 reflect a range of collision cross sections for the peaks observed at shorter drift times that are not entirely resolved. Many of these unresolved features display reproducible structure, which we have shown as the solid points that are superimposed on the lines. The smallest cross sections, observed for the +4 to +7 states, are similar to the value calculated for the crystal structure. These conformers are most abundant in data recorded after ions were exposed to proton transfer reagents (see below). We have divided the collision cross sections shown in Figure 4 into three conformation types: compact conformations, that we define as those features having a cross section below 1120 Å^2 (+4 to +7); an elongated conformation, for cross sections that are larger than 1500 Å^2 (+6 to +13); and conformations that we refer to as partially folded, having cross sections between these values.

Ion Mobility Distributions After Proton-transfer Reactions

Figure 5 shows ion mobility distributions (at an injection energy of 385 eV) for the +8 and lower charge states before and after ions were exposed to each proton-transfer base. The ion mobility distributions for the +9 and higher charge states that remain after

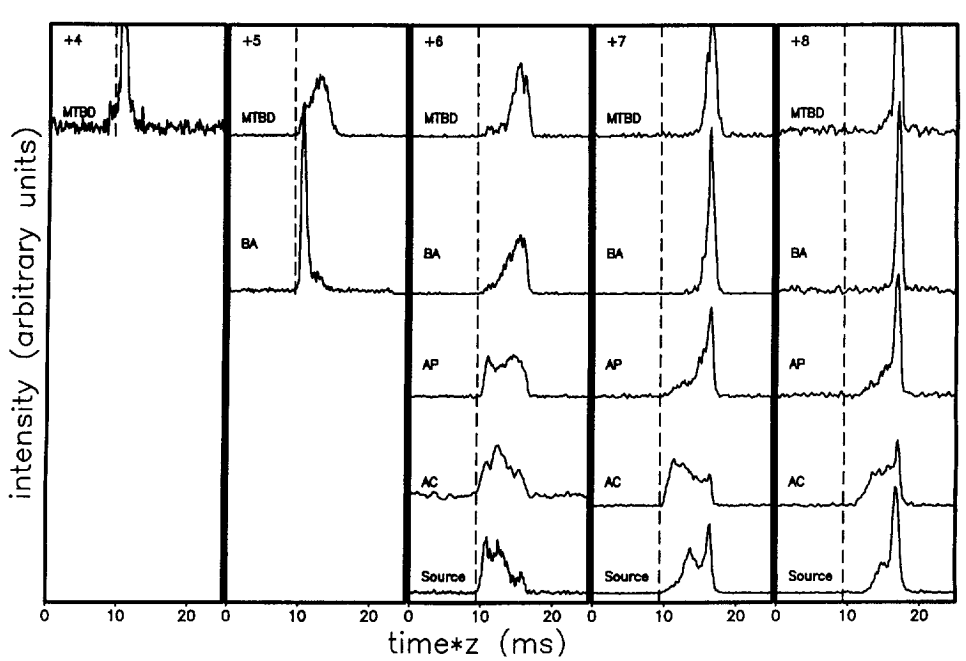

Figure 5. Charge-normalized ion mobility distributions for the +4 to +8 charge states obtained before and after proton-transfer reagents have been added to the source. The data labeled *source* correspond to distributions that were recorded before bases were added. The labels associated with the other data are for distributions that are recorded after ions have been exposed to acetone (AC), acetophenone (AP), n-butylamine (BA), and 7-methyl-1,5,7-triazabicyclo[4.4.0]dec-5-ene (MTBD). The dashed line shows the drift time that is calculated for the crystal conformer.

exposure to proton transfer reagents are indistinguishable from data recorded before bases were added. Each displays a single peak corresponding to an elongated conformer. For the +8 and lower states, the ion mobility distributions depend upon the reagent used. When acetone is added to the gas cell the relative abundances of compact and partially-folded conformations in the +7 and +8 charge states increase relative to the elongated conformation. The distribution recorded for the +6 state is similar to data recorded when no base is present, although it is possible that the fraction of partially folded conformers has increased slightly. When ions are exposed to acetophenone, the abundances of compact and partially folded conformers in the +7 and +8 charge states decrease, and elongated conformations dominate the distributions. The distribution for the +6 charge state after exposure to acetophenone shows an increase in the relative abundances of the compact and partially folded conformers.

Exposing the ions to stronger bases leads to larger changes in the ion mobility distributions. After ions are subjected to n-butylamine vapor, the +7 and +8 states display only elongated conformers. The relative abundance of compact conformers for the +6 state is decreased and this state becomes dominated by a distribution of partially folded and elongated conformers. The +5 state is not observed until addition of n-butylamine and exists almost exclusively as a compact conformation. When MTBD is added to the reaction cell, the +6 to +8 distributions are similar to the results observed with n-butylamine. The +5 state formed by reaction with MTBD is not dominated by the most compact conformer, as was observed for reaction with n-butylamine. Instead, partially folded forms are favored. MTBD is the strongest base studied here (GB = 243.3 kcal/mol) and also forms the +4 charge state, which exists as a compact conformer.

Each ion that is present after exposure to proton transfer reagents has been examined at high injection voltages. Ion mobility distributions for the +6 and higher states show a single peak corresponding to the elongated conformer, analogous to data before proton transfer reactions have occurred (Figure 3). For the +5 state at high injection energies, the distributions observed after addition of these bases are quite similar and a partially folded conformer is favored. The +4 charge state that is formed by reaction with MTBD favors a compact conformation at low and high injection energies. It is generally assumed that the most stable structures predominate in ion mobility distributions recorded at high injection energies.

Relative Gas-phase Acidities of Compact, Partially Folded, and Elongated Conformers

The dominant peak in the mass spectra (Figure 2) observed after reaction of each base is the +7 or higher charge states that are comprised primarily of elongated conformations. From the fractions of each charge state (observed in the mass spectra) and conformer abundances (obtained from the ion mobility data), the total fraction of elongated ions before addition of bases is ~85%, and after bases are added, ~85%, 90%, 85%, and 70% for acetone, acetophenone, n-butylamine, and MTBD, respectively. Within the combined uncertainties for these estimates (~15%), these values are the same, showing that there are no large changes in the fraction of elongated ions during the proton-transfer reactions. Elongated conformations can undergo proton-transfer reactions, as observed with n-butylamine and MTBD; however, the lower charge state ions that are formed appear to also be elongated (although they do contract slightly). This shows that for ubiquitin, conversion of elongated conformers into compact ones during proton-transfer reactions is insignificant. Thus, unlike ion mobility data for cytochrome *c* [12b], apomyoglobin [12d], and lysozyme [13], there is no strong evidence that ubiquitin ions undergo folding transitions in the gas phase.

A simple explanation for the data in Figure 5 is that for a given charge state, proton-transfer reactions selectively deplete the compact and partially folded conformations. This favors these conformations in lower charge states and leaves elongated forms of highly charged ions. Examples of this behavior can be observed from Figure 5 for the +7 and +8 charge states after ions have been exposed to acetophenone, n-butylamine, or MTBD. For the +6 and lower charge states formed during reactions with n-butylamine and MTBD, we observe that compact conformers are more reactive than partially folded ones. That is, the small fraction of compact conformers continues to undergo proton-transfer reactions forming the +5 state after exposure to n-butylamine, and reacts further with MTBD forming the +4 state. The partially folded +6 state appears to be largely unreactive with n-butylamine, but with MTBD the partially-folded +5 state is formed.

Although we cannot rule out a complex scenario in which some conformations interconvert during proton-transfer reactions, leading to only small changes in the total fractions of different conformations, the simplest explanation for our data is that the proton-transfer process is selective for the overall conformation. From data presented above, we predict that relative ordering of the apparent gas-phase acidities for different conformations within a given charge state is compact < partially folded < elongated.

The apparent gas-phase acidities for the +4 through +13 charge states of ubiquitin measured by Zhang and Cassady decrease with increasing charge state, a result that they explained by three considerations: the intrinsic acidities of individual deprotonation sites; total Coulomb energy; and three-dimensional conformations [8b]. The low apparent gas-phase acidities for very high charge states can be qualitatively understood by considering the intrinsic acidities of the protonated arginine, lysine, and histidine residues. The fraction of these

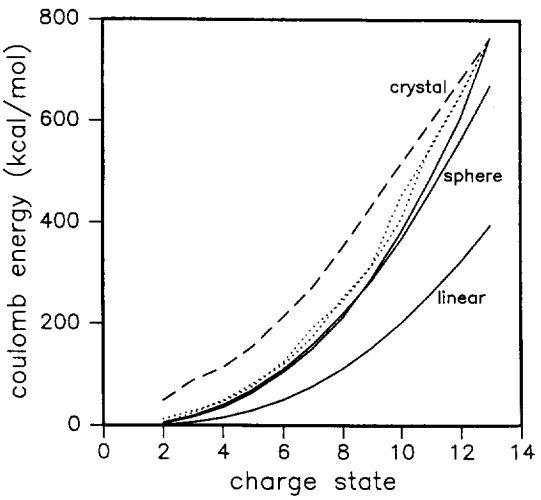

Figure 6. The solid lines show Coulomb repulsion energies for 2 to 13 charges on the surfaces of three model structures: (1) a model that assumes that charges are assigned to basic residue sites on the crystal structure; (2) a model where protons are placed in lowest energy configurations on the surface of a sphere having the average radius of the crystal structure; and (3) a model where protons are placed in the lowest energy positions on a linear string. The dashed line corresponds to protonation of sites in the crystal conformer that maximizes the Coulomb energy. The dotted lines correspond to sequential removal of protons from randomly chosen sites of the crystal structure.

protonated sites increases for high charge states, making them available during proton transfer reactions. This should lower the apparent gas-phase acidities of the high charge state ions.

From our data it appears that the dominant factor that governs the proton-transfer reactivity of ubiquitin is the conformer type. The differences in reactivity can be understood by considering the total Coulomb energies for the different conformers. Schnier et al. have discussed that as the total Coulomb energy increases, the apparent proton affinity of the ion decreases [9a]. The dielectric constants of gas-phase ubiquitin ions are unknown; however, a value of 2.0 ± 0.2 has been determined for the shielding of charges on multiply protonated cytochrome *c* [9a]. Using this value, we have calculated the Coulomb energies for different charge states of three model ubiquitin structures: (1) a model that assumes that charges are assigned to sites on the crystal structure; (2) a model where protons are placed in lowest energy configurations on the surface of a sphere having the average radius of the crystal structure; and (3) a model where protons are placed in the lowest energy positions on a linear string. The results are shown in Figure 6. Conformers with small cross sections (such as the compact sphere and crystal) possess higher Coulomb energies than those with larger cross sections. The compact conformers observed experimentally should have Coulomb energies similar to a sphere or crystal form. The elongated and partially folded conformers will have Coulomb energies that lie between values calculated for the model compact and linear forms. The driving force for the selective depletion of more compact conformers is the large drop in Coulomb repulsion for compact states as protons are removed.

We do not have a good understanding of the roles of individual charged sites during the proton transfer process. Differences in the location of charges (within a charge state and conformation type) will influence the conformation due to small differences in Coulomb energies and localized intraprotein charge stabilization factors. There are many low-energy combinations of protonated sites within a given charge state, and subtle differences in their conformations could explain the broad nature of many of the features in our ion mobility data. Figure 6 shows calculated Coulomb energies for sequentially removing protons from different sites on the crystal structure in a variety of different combinations, including those yielding the lowest and highest Coulomb energies, as well as two progressions corresponding to random removal of charges. It appears that for all charge states, protons can be removed from sites in any order and still significantly reduce the Coulomb energy. Thus, it seems unlikely that deprotonation of a specific site is required. We are currently investigating the conformations of negatively charged deprotonated ions in order to further delineate how the location of charges influences the conformations of protein ions [24].

Conclusions

The conformations and proton-transfer reactivity of ubiquitin ions have been studied using ion mobility/mass spectrometry methods. A wide range of conformations have been observed and characterized as compact, partially folded, and elongated conformer types. By comparing the mass spectra and ion mobility distributions that were recorded for ions formed directly by ESI, and data recorded after ions were exposed to acetone, acetophenone, n-butylamine, or MTBD, we have characterized the proton transfer reactivity of the different conformer types. The results are consistent with conformer-selective reactions that preferentially deplete compact and partially folded conformations. Elongated conformers are found to be less reactive and there is no evidence that these states undergo gas-phase folding reactions as protons are removed. The conformer-selective reactivities are consistent with the following ordering for the apparent gas-phase acidities within a given charge state: compact < partially folded < elongated. The origin of the differences in gas-phase acidities for the different conformer types can be understood by considering the total Coulombic repulsion energies.

Acknowledgment

The authors gratefully acknowledge the National Science Foundation (grant no. CHE-9625199) for support of this work.

References

1. Whitehouse, C. M.; Dreyer, R. N.; Yamashuta, M.; Fenn, J. B. *Anal. Chem.* **1985,** *57,* 675–679. Fenn, J. B.; Mann, M.; Meng, C. K.; Wong, S. F.; Whitehouse, C. M. *Science* **1989,** *246,* 64–71.
2. Karas, M.; Hillenkamp, F. *Anal. Chem.* **1988,** *60,* 2229. Karas, M.; Bahr, U.; Giessman, U. *Mass Spectrom. Rev.* **1991,** *10,* 335–357. Hillenkamp, F.; Karas, M.; Beavis, R. C.; Chait, B. T. *Anal. Chem.* **1991,** *63,* 1193A–1202A.
3. Winger, B. E.; Light-Wahl, J. J.; Rockwood, A. L.; Smith, R. D. *J. Am. Chem. Soc.* **1992,** *114,* 5897–5898.
4. (a) Suckau, D.; Shi, Y.; Beu, S. C.; Senko, M. W.; Quinn, J. P.; Wampler III, F. M.; McLafferty, F. W. *Proc. Natl. Acad. Sci. USA* **1993,** *90,* 790–793. (b) Wood, T. D.; Chorush, R. A.; Wampler III, F. M.; Little, D. P.; O'Connor, P. B.; McLafferty, F. W. *Proc. Natl. Acad. Sci. USA* **1995,** *92,* 2451–2454.
5. Cassady, C. J.; Carr, S. R. *J. Mass Spectrom.* **1996,** *31,* 247–254.
6. Valentine, S. J.; Clemmer, D. E. *J. Am. Chem. Soc.* **1997,** *119,* 3558–3566.
7. (a) Ogorzalek Loo, R. R.; Smith, R. D. *J. Am. Soc. Mass Spectrom.* **1994,** *5,* 207–220. (b) Ogorzalek Loo, R. R.; Winger, B. E.; Smith, R. D. *J. Am. Soc. Mass Spectrom.* **1994,** *5,* 1064–1071.
8. (a) Cassady, C. J.; Wronka, J.; Kruppa, G. H.; Laukien, F. H. *Rapid Commun. Mass Spectrom.* **1994,** *8,* 394–400. (b) Zhang, X.; Cassady, C. J. *J. Am. Soc. Mass Spectrom.* **1996,** *7,* 1211–1218.
9. (a) Schnier, P. F.; Gross, D. S.; Williams, E. R. *J. Am. Chem. Soc.* **1995,** *117,* 6747–6752. (b) Gross, D. S.; Schnier, P. D.; Rodriguez-Cruz, S. E.; Fagerquist, C. K.; Williams, E. R. *Proc. Natl. Acad. Sci. USA* **1996,** *93,* 3143–3148. (c) Williams, E. R. *J. Mass Spectrom.* **1996,** *31,* 831–842.
10. (a) Covey, T. R.; Douglas, D. J. *J. Am. Soc. Mass Spectrom.* **1993,** *4,* 616–623. (b) Douglas, D. J. *J. Am. Soc. Mass Spectrom.* **1994,** *5,* 17–18. (c) Collings, B. A.; Douglas, D. J. *J. Am. Chem. Soc.* **1996,** *118,* 4488–4489.
11. von Helden, G.; Wyttenbach, T.; Bowers, M. T. *Science* **1995,** *267,* 1483–1485. Wyttenbach, T.; von Helden, G.; Bowers, M. T. *J. Am. Chem. Soc.* **1996,** *118,* 8355–8364.
12. (a) Clemmer, D. E.; Hudgins, R. R.; Jarrold, M. F. *J. Am. Chem. Soc.* **1995,** *117,* 10141–10142. (b) Shelimov, K.; Jarrold, M. F. *J. Am. Chem. Soc.* **1996,** *118,* 10313–10314. (c) Shelimov, K. B.; Clemmer, D. E.; Hudgins, R. R.; Jarrold, M. F. *J. Am. Chem. Soc.* **1997,** *119,* 2240–2248. (d) Shelimov, K. B., Jarrold, M. F. *J. Am. Chem. Soc.* **1997,** *119,* 2987–2994.
13. Valentine, S. J.; Anderson, J.; Ellington, A. E.; Clemmer, D. E. *J. Phys. Chem.* **1997,** *101,* 3891–3900.
14. Sullivan, P. A.; Axelsson, J.; Altmann, S.; Quist, A. P.; Sunqvist, B. U. R.; Reimann, C. T. *J. Am. Chem. Soc. Mass Spectrom.* **1996,** *7,* 329.
15. Hagen, D. F. *Anal. Chem.* **1979,** *51,* 870–874. St. Louis, R. H.; Hill, H. H. *Crit. Rev. Anal. Chem.* **1990,** *21,* 321–355. von Helden, G.; Hsu, M. T.; Kemper, P. R.; Bowers, M. T. *J. Chem. Phys.* **1991,** *95,* 3835–3837. Jarrold, M. F.; Constant, V. A. *Phys. Rev. Lett.* **1992,** *67,* 2994–2997. Clemmer, D. E.; Jarrold, M. F. *J. Am. Chem. Soc.* **1995,** *117,* 8841–8850.
16. (a) Gross, D. S.; Williams, E. R. *J. Am. Chem. Soc.* **1995,** *117,* 883–890. (b) Gross, D. S.; Rodriguez-Cruz, S. E.; Bock, S.; Williams, E. R. *J. Phys. Chem.* **1995,** *99,* 4034–4038.
17. Mason, E. A.; McDaniel, E. W. *Transport Properties of Ions in Gases;* Wiley: New York, 1988.
18. The crystal coordinates for human ubiquitin (having the same sequence as bovine ubiquitin) were used for this calculation. The structure was determined by Vijay-Kumar, S.; Bugg, C. E.; Cook, W. J. *J. Mol. Biol.* **1987,** *194,* 531–544.
19. Insight II, BIOSYM/MSI, San Diego, CA, 1995.
20. Recently it has been shown that when scattering trajectories are rigorously included, the calculated collision cross section can increase by as much as ~20%; Shvartsburg, A.; Jarrold, M. F. *Chem. Phys. Lett.* **1996,** *261,* 86–91.
21. Lias, S. G.; Liebman, J. F.; Levin, R. D. *J. Phys. Chem. Ref. Data* **1984,** *13.*
22. Gas-phase basicity values for all bases used in this study are taken from ref 21 unless otherwise noted.
23. Decouzon, M.; Gal, J. F.; Maria, P. C.; Raczynska, E. D. *Rapid Commun. Mass Spectrom.* **1993,** *7,* 599–602.
24. Liu, Y.; Valentine, S. J.; Clemmer, D. E., unpublished.